WORLD CONFERENCE ON TIMBER ENGINEERING 2025
BRISBANE, AUSTRALIA
Advancing Timber for the Future Built Environment

COMPRESSIVE LOADING TEST AND BURNING TEST OF STEEL BAR-TIMBER COMPOSITE COLUMNS

Rin Kamimakise[1], Toshihisa Ishii[2] , and Shinichi Shioya [3]

ABSTRACT: We have been developing a frame system consisting of steel bar-timber composite members which can perform better than those of reinforced concrete structure. The steel bar is deformed bar, which is embedded near outer in the cross-section of the composite member and bonded with epoxy resin adhesive. Bending stiffness of the composite member is estimated to be approximately five times that of conventional glulam timber for beam and approximately twice for column. Also, the bending strength capacity of the composite member is estimated to be approximately three times for beam and approximately twice for column. Compression tests were conducted to estimate the compression capacity of columns, including buckling capacity, and 90-minute heat tests under loading were conducted. This paper presents the experimental tests, their results, and estimations of the capacities.

KEYWORDS: Glulam timber, Composite member, Column, Compressive capacity, Buckling capacity

1 – INTRODUCTION

Nowadays cross laminated timber (CLT) is being used for building. However, CLT often restricts the planning of buildings because it is flat plate member. In order to improve the flexibility of the planning, higher stiffness and strength are desired for column and beam. We have been developing a frame system formed with steel bar-timber composite members which can perform better than those of reinforced concrete structure[1]. The steel bars are deformed bar (hereinafter referred to as "rebar") which are embedded near outer in cross-section of the composite member and bonded with epoxy resin adhesive. The bending stiffness of the composite member is estimated to be approximately five times that of conventional glulam timber for beam and approximately twice for column. Also, the bending strength of it is estimated to be approximately three times for beam and approximately twice for column. Compression tests were conducted to estimate the compression capacity of columns, including buckling capacity, and also 90-minute heat tests under loading were conducted. This paper presents the experimental tests, their results, and estimations of the capacities.

2 – BACKGROUND

In 2016, a factory building with a 20-m-span Two-way frame was built using the system developed by S. Shioya; in 2018, a factory building with a 25-m-span one-way frame was built using this system; in 2020, it was used in a trial for the top floor of a new 11-story high-rise building in Tokyo, meeting the requirement of being fireproof for up to two hours of burnning. The composite column replaces concrete with wood, which reduces the weight of building and results in superior seismic performance. While some studies have been reported on other timber composite members mainly for beam members, no studies has been reported on those for columns, except for the study by S. Shioya et al. Shioya et al. conducted horizontal force tests on the steel bar-timber composite column connected to reinforced concrete foundations and reported that the columns showed superior performance to reinforced concrete columns in terms of stiffness, bending capacity, energy dissipation, damage control, and ductility[1]. Furthermore, the authors report the bending performance in the range from low to high axial forces in the sections that do not yield in bending and those that do yield in bending, as well as the bending stress characteristics and methods for estimating stresses.[2]. Remaining issues to be investigated, with respect to the column, are the compressive capacity of long columns, including buckling, and estimation method for it, and the design of column under fire by the use of burning marginal layer.

3 – COMPRESSIVE LOADING TEST

[1] Rin Kamimakise, Department of Architecture, Kagoshima University, Kagoshima, Japan, k6194691@kadai.jp

[2] Toshihisa Ishii, Department of Architecture, Kagoshima University, Kagoshima, Japan, k3431122@kadai.jp

[3] Shinichi Shioya, Department of Architecture, Kagoshima University, Kagoshima, Japan, k7347039@kadai.jp

https://doi.org/10.52202/080513-0119

3.1 SPECIMEN

Figure 1 shows the cross-section of a specimen. There were two types of specimens: conventional glulam timber (WO) and reinforced laminated timber (HW). The scale is approximately 1/4 of the actual size. The reinforcement ratio to gross section p_g is 5.64%. The specimens were divided into two types: those used to investigate the compression characteristics of the column without causing buckling (WO-S, HW-S) and those used to investigate the buckling resistance of the column (WO-L, HW-L). Table 1 shows a list of long column specimens. The length L of the specimen and the buckling length Lk are listed. The glulam was made of Japanese cedar of the same grade (E65-F255, all lamina grade L70), and the rebar was SD345 with D13 of diameter. The construction of the specimen is the same as described in the literature[3]. The upper and lower loading surfaces of the short column specimens (WO-S, HW-S) were machined on a milling lathe to ensure flatness, and the long column specimens to be buckled could not be installed on the milling lathe, so the upper and lower surfaces of the columns were capped with the epoxy resin adhesive used to bond the rebars.

Table 1: *Size and slenderness ratio of long column specimens*

Specimen		WO-L-1500	WO-L-2000	WO-L-2500	WO-L-3000-1	WO-L-3000-2
L	in mm	1313	1813	2316	2715	2714
L_k	in mm	1499	1999	2502	2901	2900
I	in mm^4	2.16x10^7	2.16x10^7	2.16x10^7	2.16x10^7	2.16x10^7
A	in mm^2	1.80x10^4	1.80x10^4	1.80x10^4	1.80x10^4	1.80x10^4
i	in mm	34.6	34.6	34.6	34.6	34.6
$\lambda=L_k/i$		43.3	57.7	72.2	83.7	83.7
Specimen		**HW-L-1500**	**HW-L-2000**	**HW-L-2500**	**HW-L-3000**	
L	in mm	1314	1814	2227	2713	L : Length of specimen
L_c	in mm	1235	1739	—	—	L_c: Length after the ends of specimen cut
L_k	in mm	1421	1925	2413	2899	L_k : Length for buckling
I_e	in mm^4	5.88x10^7	5.88x10^7	5.88x10^7	5.88x10^7	I, I_e : Moment of inertia area
A_e	in mm^2	4.90x10^4	4.90x10^4	4.90x10^4	4.90x10^4	A, A_e : Cross arae
i_e	in mm	34.6	45.8	45.8	45.8	i : Secondary radius of section
$\lambda_e=L_k/i_e$		41.0	55.6	69.7	83.7	
A_u	in mm^2	3.62x10^4	3.62x10^4	3.62x10^4	3.62x10^4	
i_u	in mm	45.8	45.8	45.8	45.8	
$\lambda_u=L_k/i_u$		31.0	42.1	52.7	63.3	

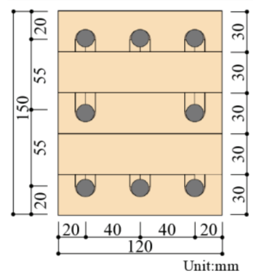

Figure 1: *Cross-section*

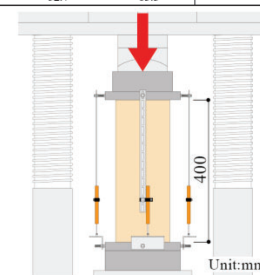

Figure 2: *Set-up for loading*

3.2 COMPRESSION OF SHORT COLUMN

Figure 2 shows the side view of the specimen, the loading situation, and the deformation measurement situation. There were three specimens of laminated wood (WO-S) and two of reinforced laminated wood (HW-S). They were installed in a compression resistant testing machine and subjected to unidirectional compression loading. Their failures were the same as those in the literature [3]. Figure 3 shows the compression stress-strain relationship. The vertical axis is the stress obtained by dividing the compressive load by the cross-sectional area (BxD) of the column. HW-S has increased elastic stiffness and compressive strength compared to WO-S, and the strain range at which the compressive strength can be maintained (hereafter reffered to as the limit strain) has also increased. Table 2 shows the experimental results.

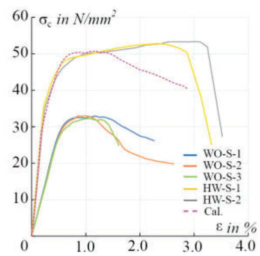

Figure 3: *Compressive stress-strain curves*

Table 2: *Experimantal results*

Specimen	N_y	N_m	σm	Ewc
	in kN		in N/mm^2	
CW-S-1	470	607	33.7	7,750
CW-S-2	470	603	33.5	8,125
CW-S-3	440	589	32.7	7,500
CR-S-1	700	1020	56.7	18,095
CR-S-2	690	1004	55.8	19,250

Note, N_y:Yield Force, N_m:Axial capacity
σ_m:Compressive strength
E_{wc}:Young's modulus

3.3 BENDING OF LONG COLUMN

The longest column specimens were subjected to four-point bending loading. One of the glulam column specimens was loaded to failure to investigate the bending strength of laminated wood. This specimen is named as WO-L-3000-0. WO-L-3000-1, WO-L-3000-2 and HW-L-3000, were loaded within the elastic region to investigate bending stiffness only. Figure 4 shows the loading situation and the measurement of deformation and strain. Table 5 shows the experimental values.

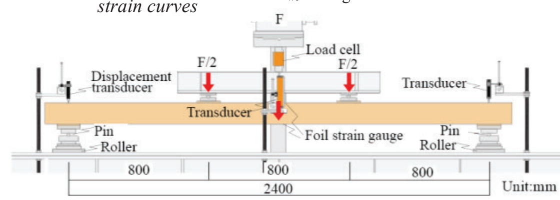

Figure 4: *Set up loading and measurement of deflection and strain*

Table 3: *Experimental results of long column by bending loading*

Specimen		WO-L-3000-0	WO-L-3000-1	WO-L-3000-2	HW-L-3000
EI	kN m^2	1.645×10^{11}	1.640×10^{11}	1.672×10^{11}	3.949×10^{11}
E_w	N/mm^2	7379.28	7542.31	7910.23	–
Average	N/mm^2		7610.606		–
M_{max}	kNm	159.5	–	–	–
F_{wb}	N/mm^2	43.3	–	–	–

EI: Bending stiffness, Ew: Young's modulus of timber, Mmax: Bending moment capacity, Fwb: Bending strength of timber

3.4 COMPRESSION OF LONG COLUMN

3.4.1 Loading

Specimens and column lengths are listed in Table 1. Figure 5 shows the rebar detail at the top and bottom of the column of HW specimen. The distance between the rebar and the end of the column was 27.5 mm. It was predicted that the maximum load would increase as the length of the column decreased, and that the wood between the ends would fail in compression. As shown in Photo 1, the ends of the column were restrained by placing steel plates on all four sides of the column and then passing three steel plates with a square hole in the center through the column at regular intervals (50 mm). Figure 6 shows the loading conditions. Figure 7 shows the upper and lower support conditions. Two-way pins were installed on the upper and lower surfaces of the specimen to absorb the tilt errors that occurred during fabrication. The buckling length L_k is the vertical distance between the upper and lower one-way pins.

https://doi.org/10.52202/080513-0119

3.4.2 Cutting the ends of the timbar

In the specimen with the longest length (HW-L-3000), the ends of timber were not damaged, and the center height of the column bent and buckled, but in the specimen with shorter length of timber (HW-L-2500), as shown in Photo 2, the timber ends were crushed in compression at maximun load and the load stopped increasing. The strengthening in Photo 1 was inadequate. In HW-L-1500 and HW-L-2000, the timber ends on both sides were cut with an electric saber saw at the cross section position where the rebar resisted compression at the ends. As a result, their column lengths were shortened from the initial length. The length L_c is shown in Table 1. Again, the flatness of the cut end surface was somewhat disturbed, as shown in Photo 3. Adverse effects of this cutting will be discussed later.

3.4.3 Experimental results

Photo 4 shows two columns after buckling. Figure 8 shows the relationship between the compressive load and the horizontal deformation of the center height of the column. The column bent due to buckling just before the maximum load, and the horizontal deformation increased.

3.4.4 Estimation of buckling strength

The experiments are shown in Table 4. Table 1 also shows the slender ratio λ_e using the equivalent bending stiffness. The relationship between the compressive stress at the maximum load and the slender ratio is shown in Figure 9 with pink and light blue solid lines. The compressive stress was calculated by dividing the maximum load by the cross-sectional area of the column (BxD) ignoring the rebars. The curves are obtained by taking the average compressive strength of the short column specimens as the compressive strength of the short column. For WO, the experimental values were estimated using the light blue dotted curve for λ values of 57.5 or more, and for HW, the experimental values were estimated using the curve for λ values of 69.7 or more. In the inelastic buckling region ($\lambda \leq 57.7$), the calculated values of the reduction factor curve for WO almost match the experimental values '○' but for HW the experimental values '○' are smaller than the calculated values of the reduction factor curve. The reason for this is the effect of the aforementioned loss of flatness of the cross-section. Symbols '●' are the data for the specimens that was recently added. The end faces of the column were carefully cut and then epoxy adhesive was used to cap them. The end faces did not crushed at all during loading. The problem of the flatness has been solved. The data λ_e=41.0 is close to the stress intensity of the pink-solid curve. In the specimen λ_e=55.6, the horizontal deformation of the mid-height of the column was relatively large from the beginning of loading, so there is a possibility that an initial error in set of the specimen to the appartusng occurred. Further experiments are needed. The dotted line is the curve used in the design. The compressive strength of the wood was assumed to be 20.6N/mm^2 and the yield strength of the rebar was assumed to be 345N/mm^2. These are the standards for the materials. The curves of the design values are on the safe side compared to the experimental values.

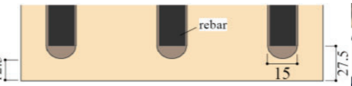

Figure 5: *Rebar's end in column specimen*

Photo 1: *Strengthing of column's end*

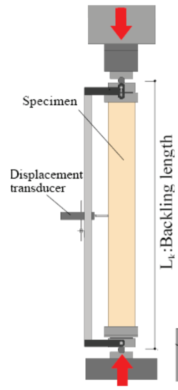

Figure 6: *Set up for loading*

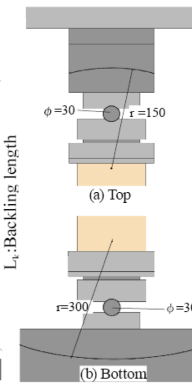

Figure 7: *Details of support of column's end*

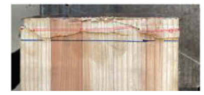

Photo 2: *Crushing of wood after loading*

Photo 3: *Non plane of column's end cut*

Photo 4: *Bending with backling*

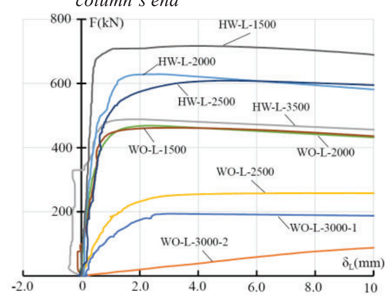

Figure 8: *Force-lateral disp. curves*

Table 4: *Experimental results of long column by axial loading*

Specimen	WO-L-1500	WO-L-2000	WO-L-2500	WO-L-3000-1	WO-L-3000-2
$\lambda = L_k/i$	43.3	57.7	72.2	83.7	83.7
N_y kN	375.0	388.0	200.0	170.0	—
N_{max} kN	461.4	468.3	257.7	193.8	—
Specimen	**HW-L-1500**	**HW-L-2000**	**HW-L-2500**	**HW-L-3000**	Ny: Axial load at rebar yielding Nmax: Maximum axial load capacity
$\lambda_e = L_k/i_e$	41.0	55.6	69.7	83.7	
N_y kN	620.9	559.1	603.2	440	
N_{max} kN	716.9	608.9	628.4	488.1	

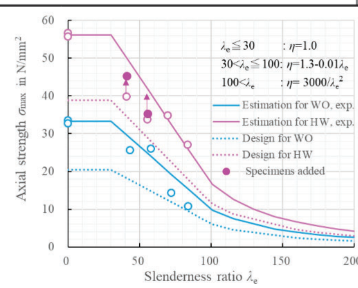

Figure 9: *Compressive strength-slenderness relationship*

4- 90-MINUTE BURNING TEST

4.1 SPECIMEN

Figure 10 shows two cross-sections of specimens. The smaller cross section (cross section A) is for the first floor

https://doi.org/10.52202/080513-0119

column of a three-story building, and the larger cross section (cross section B) is for that of a four-story building. The solid red line on the cross section indicates the secondary bonding line at the time of manufacture. When a building is completely collapsed by fire, the building is removed, but in reality, firefighting often results in only partial burning of the building. In this case, the building must be reused by repairing the burned portion. If the columns burn and the weight of the upper floors causes the floors of each floor to fall vertically, repairs will be difficult. In particular, it is desirable to design the fire resistance of columns on the first floor of multi-story buildings to withstand a longer burning time than time legally required against local fires in building.
In the case of steel bar-timber composite column, heating causes the rebar to expand axially and buckle easily. The strength of the adhesive bonding the rebar also decreases rapidly at 70-100°C. Once the rebar has buckled, the columns become extremely difficult to repair. Therefore, the time when the wood around the rebar placed around the perimeter of the column cross- section reaches the charred boundary should be considered as the time when repair becomes impossible (repair limit time).
As is natural, even if the rebar buckles, the larger cross-sectional area except the burned-out portion will still be resistant, so the fire resistance time to support long-term loads is still long. In the cross section in Figure 11, the repair limit time is increased by increasing the thickness of the wood as fireproof covering around the structural cross section (area enclosed by the blue line). As a guide, the repair limit time is set at 60 minutes and the fire resistance time is set at 90 minutes. The spacing of the rebars in Figure 8 is determined laterally by the restrict of the joint (Splice sleep mortar-filled joint) between the rebars of the first-story column and the rebars of the reinforced concrete foundation, and vertically by the restrict of the thickness of the lamina used.

4.2 CALCULATION CONCEPT FOR COL-U MN CAPACITY

1) Resisiting portion expected within a column cross-section after 75 minutes of burning is shown in Figure 11(a). A four-story wooden building that can be designed using the current semi-fireproof design method requires a fire resistance time of 75 minutes. In this case, cladding layer (gray area) of 65 mm is required in Japan. The expected axial strength of a column is the axial strength calculated as if the wood and rebars in the remaining portion of the column, excluding its burnned depth, can resist under the allowable stress in short-term loads.
However, since the rebar becomes hot when the charred boder contacts the rebar, the wood around such rebar must not resist within a certain range of dimensions. he range is shown in Figure 11(b). The rebar shall also not resist. Since the temperature limit of the glue used for the rebar is low (70-100°C), its contact with the charred boundary is determined by the depth of the wood to the outer circumference of the hole in the rebar. Rebar whose charred boundary does not touch the hole is able to withstand the short-term allowable unit stress.
2) Young's modulus of the wood portion in the area 45mm from the charred border to the uncharred portion

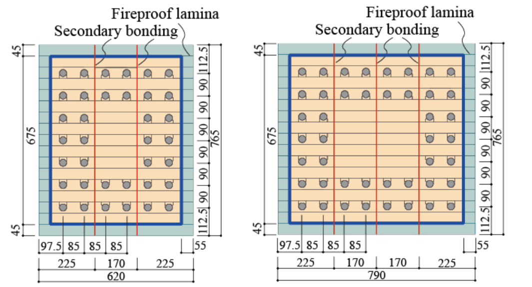

(a) Cross section A (b) Cross section B

Figure 10: *Cross-section*

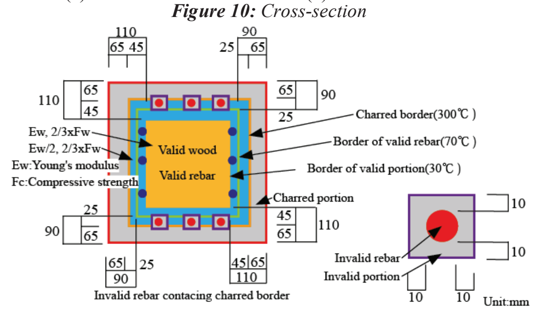

(a) Invalid and valid portions (b) Invalid portion around rebar contacting charred border

Figure 11: *Valid portions in cross-sections of specimen for resisting*

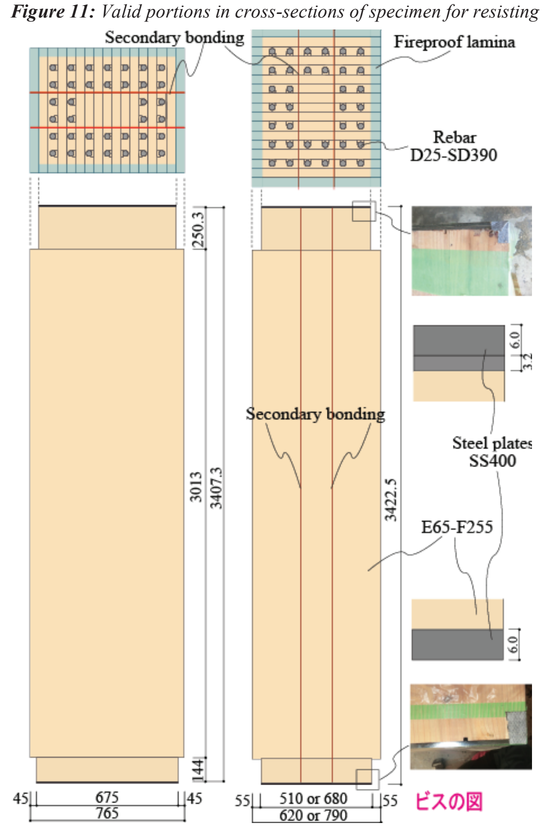

Figure 12: *Side views of Specimen A and details of ends of column*

(the blue area in Fig. 11(a)) is set to 50% of the standard, and the Young's modulus Ew of the wood in the area further inside is set to Ew, and the slender value of the buckling reduction factor of the column is calculated.

4.3 COMBUTION OF COLUMN

4.3.1 Specimen

Two types of column cross-sections are shown in Fig.10. Two specimens of cross section A and one specimen of cross section B were planned, and a loading heat combustion test of one specimen of both cross sections was first conducted on August 16, 2024. The specimens of each cross section are designated as A1 and B1. Another specimen of cross section A was conducted on December 19, 2024, and its name is A2. In A1 and B1, only the temperature and strain of wood were measured, while, in A2, the temperature and strain were measured in detail, including rebars. Comfigration of the specimens is shown in Figure 12. To ensure the flatness of the applied force surface, 6mm thick steel plates were screwed into the upper and lower structural sections of the specimen. The heads of the screws were placed within the thickness of the steel plate. Table 5 and Table 6 show material mechanical properties of wood and rebar. Table 7 shows the performance of the adhesives used to bond the rebars to the lamina. The upper limit of the working temperature of the adhesive is 70°C.

4.3.2 Load carrying capacity and bearing capacity after 75 minutes of combustion

The allowable compressive strength capcity of the column in long-term load was loaded to the top of the column. The capacity was determined by the long-term allowable compressive stress of rebar (D25) (=215N/mm^2). The stress of wood was assumed to be 6.81 N/mm^2. This value is 90% of the long-term compressive allowable stress of wood, which is 7.6 N/mm^2. Even during combustion, the strength was determined by the short-term allowable unit stress of the steel rebar (390 N/mm^2),ande the stress of the wood was assumed to be 12.37 N/mm^2. This is 90% of the short-term allowable compressive unit stress of the wood (13.7 N/mm^2). The calculation of strength is the same as the calculation of the long-term allowable strength.

Table 8 shows the calculated long-term allowable compressive strength capacity N_L of the columns and the calculated short-term compressive strength capacity N_{FS} expected after 75 minutes of burning. In all cases, the slenderness ratio based on the equivalent cross-section is less than 30, and the buckling reduction factor η is 1.0, so it is determined that buckling would not occur. Nu1 and N_{u2} are calculated values for the ultimate strength after 75 minutes of burning. N_{u1} is done using standard values of wood and rebar, and N_{u2} is done using strengths of material testi. The loading during the combustion test is 1.05 times the N_L for each specimen. Specimens A1 and A2 were loaded to 6450 kN and B1 was loaded to 8150 kN, maintaining the loads for each combustion.

Table 5: *Mechanical properties of timber for compression*

E_{wc}	F_{wc}
6063	36.4

Unit:N/mm^2

E_{wc} and F_{wc}:Young's modulus and strength by compressive test

Table 6: *Mechanical properties of rebar*

Rebar	E_r	σ_y	σ_{tu}
D25	1.81×10^5	422.1	606.9

Er:Young's modulus, σ_y:Yielding strength, σ_{tu}:Braking tensile strength

Nominal diameter and cross area of rebar: 25mm, 506.7mm^2

Table 7: *Properties of Epoxy resin adhesive*

Strength in N/mm^2				Tensile Elastic Modulus in N/mm^2
Compressive	Tensile	Bending	Tensile shear	
76.4	43.4	64.9	20.4	2200

Table 8: *Calculation of compressive strength capacities of specimens*

Specimen	B	D	Bs	Ds	N_L	N_{FS}	N_{U1}	N_{U2}
	mm				kN			
A	765	620	675	510	6136	8218	9336	13520
B	765	790	675	680	7757	11121	12873	18685

B, D, Bs, Ds : See Fig .3, N_L: Allowable compressive strength for the long term

N_{FS}: Allowable compressive strength for burning using the short term strength

N_{U1}: Ultimate compressive strength for burning using standard strength of E65-F255

N_{U2}: Ultimate compressive strength for burning using strength of lamina's test

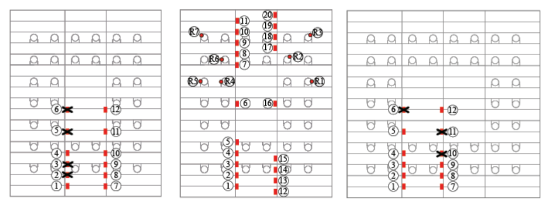

Specimen A1 Specimen A2 Specimen B

(a) Thermocouples

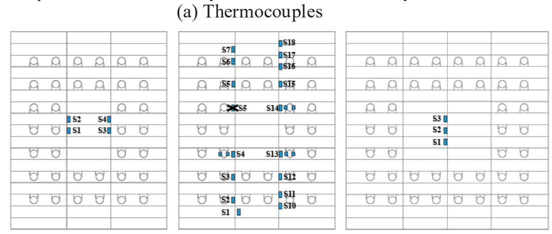

Specimen A1 Specimen A2 Specimen B

(b) Strain guage

Figure 13: *Locations of thermocouples and strain guage*

(a) Grooves for lead wires on timber (b) Lead wires from column's base end

Photo 5: *Grooves for lead wires and pulling out of them from column end*

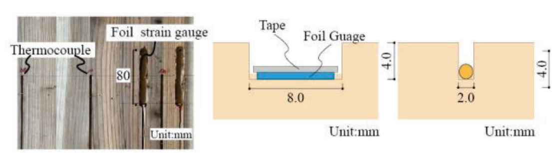

(a) Settelement into groove (b) Foil strain gauge (c) Thermocouple

Figure 14: *Enbedment of foil guage and thermocouple*

4.3.3 Measurements

Figure 13 shows the locations of thermocouples and strain gauges. They were placed at the middle hight of the columns. The lead of the strain gauge (length: 60 mm)

https://doi.org/10.52202/080513-0119

had a 3-wire type lead with the temperature compensation. locations where measurements could not be taken due to mistake of wire connection are marked with an X. The thermocouple and foil gauge were embedded in a groove machined on the secondary bonding surface before secondary bonding as shown in Figure 10. The thermocouple and foil gauge leads were glued along the groove provided for the leads as shown in Photo 5(a) and pulled out from the bottom of column as shown in Photo 5(b). As shown in Figure 14(c), a groove was cut in the secondary bonding surface of the wood to embed the thermocouple and lead wires. Vertical load and vertical deformation of the column head were measured.

4.3.4 Relationship between force and strain when introducing long-term load

Figure 16 shows the relationship between load and strain at load introduction for A2, where temperature and strain were measured in detail. the relationships for wood and rebar are shown separately. The relationship for wood is shown in Figure 16(a) and Figure 16(b), and that for rebar is shown in Figure 16(c). For wood, the calculated axial stiffness of the red single-dashed line is in close agreement with the experimental stiffness. For rebar, the experimental stiffness is smaller than the calculated value. The reason for this is unknown at this time.

4.3.5 Results of combution test

The first phase of the combustion test was conducted at room temperature 36.8°C, and the second phase was done at room temperature 12.0°C. Heating was started 5 minutes after the loading was completed. Figure 17 shows the temperature history in the furnace. Heating followed the ISO843-1 heating curve. Figure 18 shows a set up for loading. The buckling length is 3500 mm. Figure 19 shows change in force during heating as a solid red line, and the other solid lines indicate change in axial strain of wood inside the column. The wood strain in compression increased up to 70 minutes after the start of burning because the resisting cross-sectional area of wood decreased as the burning progressing, but the compressive strain began to decrease from 80 minutes as the temperature inside the column began to rise and the wood and rebar began to expand. Specimen A had a smaller volume than Specimen B, so the reduction in strain during the inversion of strain change was relatively larger.

Specimen A1 began to take out the sound of the rebar buckling at 110 minutes. The times where the sound could be confirmed is indicated by a solid circle in Figure 19. For this specimen, the furnace temperature reached the upper

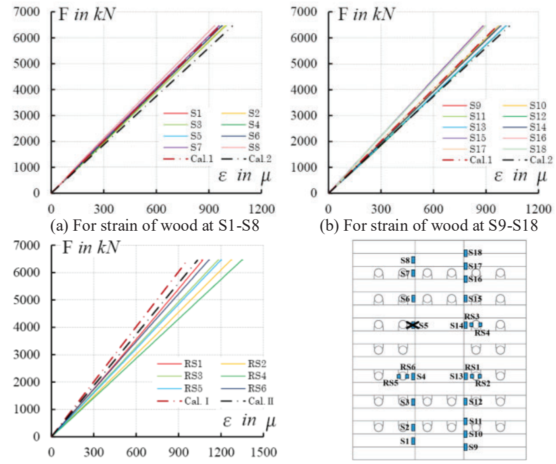

(a) For strain of wood at S1-S8 (b) For strain of wood at S9-S18

Figure 16: Compressive force-wood strain relationship of A2 during introducting force

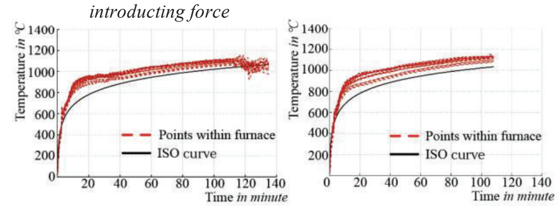

(a) Specimen A1 (b) Specimen B1

Figure 17: Temprature changes in furnace during burning

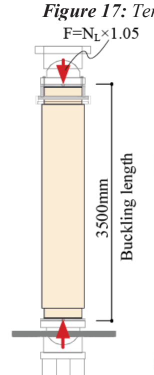

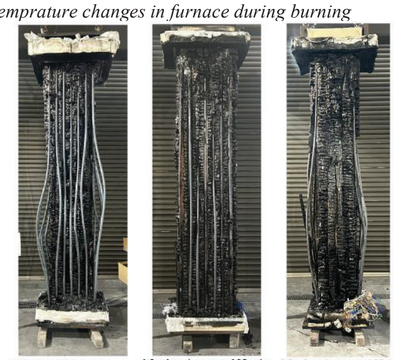
After burning up to 135 minutes under F=6446kN
(a) Specimen A1
After burning up to 108 min under F=8166kN and next reloading up to 9502 kN
(b) Specimen B1
After burning up to 108 min under F=6446kN and next reloading up to 9483 kN
(c) Specimen A2

Figure 18: Set up for loading *Photo 6: Specimen after experiment*

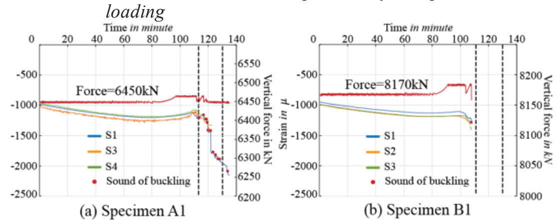

(a) Specimen A1 (b) Specimen B1

Figure 19: Changes of axial force and strain of timber during burning

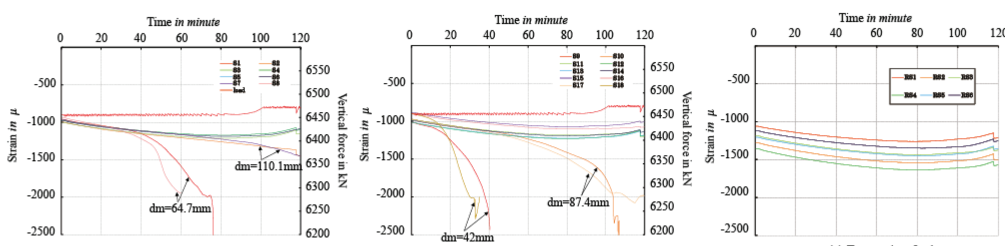

(a) For strain of wood at S1-S8 (b) For strain of wood at S9-S18 (c) For strain of rebar

Figure 20: Changes of force, axial strain of timber and rebar of Specimen A2 during burning

temperature limit after 135 minutes of heating, and heating was terminated. At that time, the specimen was still capable of supporting the initial load (F=6446 kN). Specimen B1 began to buckle at 105 minutes and was heated to 108 minutes, 1.2 times 90 minutes, and then the heating was stopped, the furnace door was opened, the flame was extinguished by discharging water, and the force was applied up to 9502 kN, which was close to the maximum load capacity (10,000 kN) of the loading system. During the loading process, many rebars were observed to buckle.

Figure 20 shows change in load during heating of A2 with solid red lines, and the other solid lines show changes in axial strain of the wood and rebar. The strain in the wood increases at shallow embedment depths (e.g., S1, S2, S7, and S8, dm=64mm and 110mm) due to the development of the charred region. Excluding these, the trend of change is similar to that of A1 in Figure 19(a). The specimens after the end of the applied force are shown in Photo 6. Specimen A1 was heated almost 30 minutes longer than Specimen B1, resulting in more severe buckling of rebars. The buckling of the rebars caused the charred layer on the surface of the column to delaminate. Both specimens satisfied the criteria for a semi-fire resistant with a fire resistance time of 90 minutes.

4.3.6 Start time of buckling

The times when the charred border of wood is assumed to reach the shortest depths to the surface and center of rebar in the column cross section is calculated to be 113 and 130 minutes, respectively based on the assumption of from the chharring rate (45/60 = 0.75 mm/min) .The times are shown by the black vertical dotted line in Figure 19. The times at which bucklings of rebar began are concentrated approximate from 113 minutes to 130 minutes, which are the calculations of the charred border reaching the shortest depth to the surface of the rebar. The repair limit time is suggested to be able to estimate as the time when the charred border reaches the depth of the rebar surface.

4.3.7 Temperature change during combustion test

Figure 21 shows the relationship between the temperature at each measuring point inside of the specimen and the heating time (hereinafter referred to as "temperature change"). The dotted curves in each color indicate the temperature change in the experiment. Figure 25 shows the depth of the thermocouple groove from the side of the specimen. The value of d_m in the figure is the minimum depth from d_{m1} to d_{m4}. Figure 22 shows the range up to 300°C. The dotted curves indicate the change in the experiment, and the solid curves in each color are the curve (Cal.) calculated on the basis of the temperature estimation described in the next section.

As wood is a natural material and non-uniform, glulam wood is composed of laminas with alternating grain orientations, and the temperature is temperature of a point, it is necessary to analyze the temperature trends on the basis of the assumption that the conditions of the material around the measurement point are somewhat different each and that there is some variation in the temperature data. Points 1 and 7 at d_m=42 mm in B1 reach 300°C in 45 minutes earlier than the points at d_m=42 mm in A1 and A2. Otherwise, the temperature increase at each point is slower as d_m increases.

5-ESTIMATION OF TEMPERATURE WITHIN CROSS SECTION

If temperature profile inside a column at any time during combustion can be estimated, the axial strength capacity of the column at the time can also be calculated. Shioya et al. proposed a method for estimating the temperature profile in a cedar glulam timber beam heated in three directions at any time during a combustion test[3]. The proposed method is based on temperature changes at limited numbers of measuring points in a specimen burned, and some constants are specified in the proposed estimation equation. For colum subjected to four way burning, the method can be used to estimate the temperature profile in the column by identifying the constants of the estimation equation based on the temperature change at several measuring points.

5.1 ASSUMPTION

The porposed method[3] was developed to be applied to the case of three-direction heating in beam. Here, 1) and 2) below are modified to apply the method to columns heated in four-directions.

1)The four sides of the column are assumed to be heated under the same conditions.

2)Figure 25 shows the symbols (d_{mx1}, d_{mx2}, d_{my1}, d_{my2}) for the distances from each side of the column to a point m within the column section. The distances are ,herein, definied collectively as d_m. The difference in the component of temperature rise due to heating from the four directions is assumed to depend only on the magnitude of d_m.

3)Temperature T at all locations in a specimen before heating shall be the same as the room temperature Tr in the combustion test, and the charring temperature Tc shall be 300°C. The range of temperatures to be estimated shall be from Tr to Tc.

4)In the range of 110-150°C at each point, the rate of temperature increase slows down as the moisture in the wood evaporates, so the charring rate is assumed to be reduced by half.

5)In actual heating, carbonization of the column surface does not occur simultaneously with the start of heating. There will be a difference between the two times. Ignoring the difference, the start of heating is assumed to be the start of carbonization of the column surface. This causes errors in the estimated temperatures at points near the surface. However, in a semi-fireproof design this is not a problem, because the column surface has already been charred near the end of heating..

https://doi.org/10.52202/080513-0119

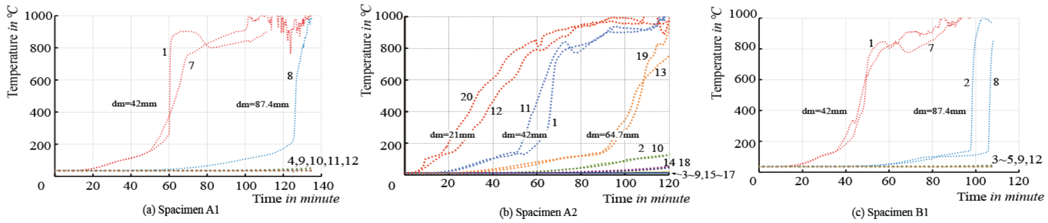

Figure 21: *Temperature of wood-time relationship of specimen/ A1,A2and B1 during heating up to 1000 ℃*

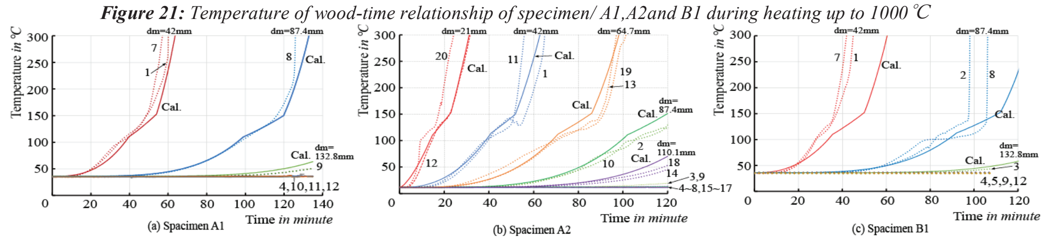

Figure 22: *Temperature of wood-time relationship of specimen/ A1,A2and B1 during heating up to 300 ℃*

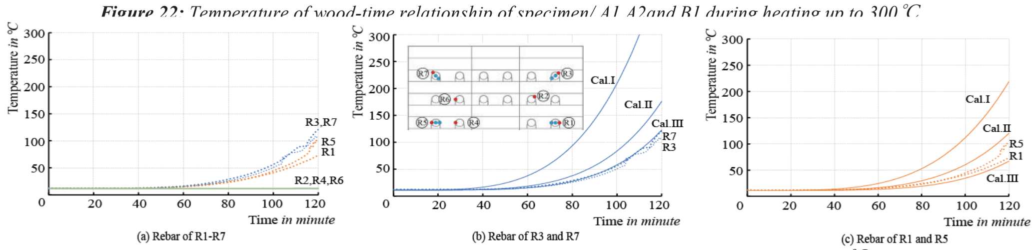

Figure 23: *Temperature of rebar-time relationship of specimen A2 during heating up to 300 ℃*

5.2 TEMPERATURE ESTIMATION EQUATION

In the basis o f the proposed method, the founction for estimating the temperature profile of wood in the cross section of a column with four-direction heating can be expressed as Equation (1).

$$T=T_r+(T_c-T_r)\{(v_c t/d_{mx1})^{Ad_{mx1}^{B}}+(v_c t/d_{mx2})^{Ad_{mx2}^{B}}+(v_c t/d_{my1})^{Ad_{my1}^{B}}+(v_c t/d_{my2})^{Ad_{my2}^{B}}\} \quad (1)$$

v_c: charring rate (mm/min), t: heating time (min)

5.3 RATE OF TEMPERATURE INCREASE

By slowing the charring rate for 110-150°C, the charring temperature will not be reached in the time of d_m/v_c. Therefore, it is necessary to accelerate the rate of temperature increase above the upper temperature of 150°C. The rate of this acceleration is β, which is expressed in Equation (2).

$$\beta=\{t_c-\alpha\,(t_{vaU}-t_{vaL})-t_{vaL}\}/(t_c-t_{vaU}) \quad (2)$$

$t_c=d_m/v_c$, t_{vaL},t_{vaU} : upper and lower limits for vaporization

5.4 COMPARISON OF CALCULATIONS AND EXPERIMENTS OF TEMPERATURE

The charring rate vc to reach the charring temperature of 300°C was assumed to be 0.65 mm/min for A1 and A2 and 0.7 mm/min for B1, based on Figure 22. The values of A and B of the constants in Equation (1) were adapted to the temperature change of specimen A2 in Figure 22(b), and the specified constants are shown in Table 5. The

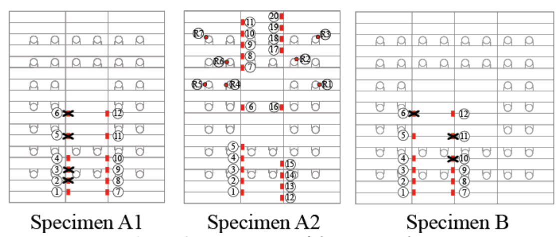

Figure 24: *Locations of thermocouples*

Table 9: *Specimens's properties and coeffients for temperature*

Specimen	Tree species	CR (mm/min.)	A	B	α	Tempreature of vaporization
Specimen A1,A2	C.J.	0.65	0.288	0.607	0.5	110-150℃
Specimen B	C.J.	0.70	0.288	0.607	0.5	110-150℃

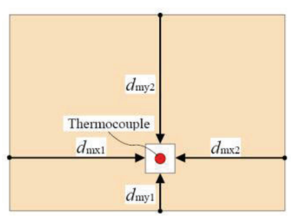

Figure 25: *Depths of d_{mx1}, d_{mx2}, d_{my1}, d_{my2} in cross section of column*

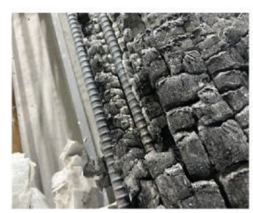

Photo 7: *Charred surface of timber after burning test*

values of d_{mx1}, d_{mx2}, d_{my1} and d_{my2} in Equation (1) are the shortest distances to the groove for thermocouple in each direction. The calculated temperature cahnge curve Cal. is shown by the solid curve.The temperature at the measuring points with d_m less than 87.4 mm clearly increase, but at deeper points, i.e. d_m greater than 110 mm, there is almost no temperature increase, so that the calculated curves also show almost no increase. Except

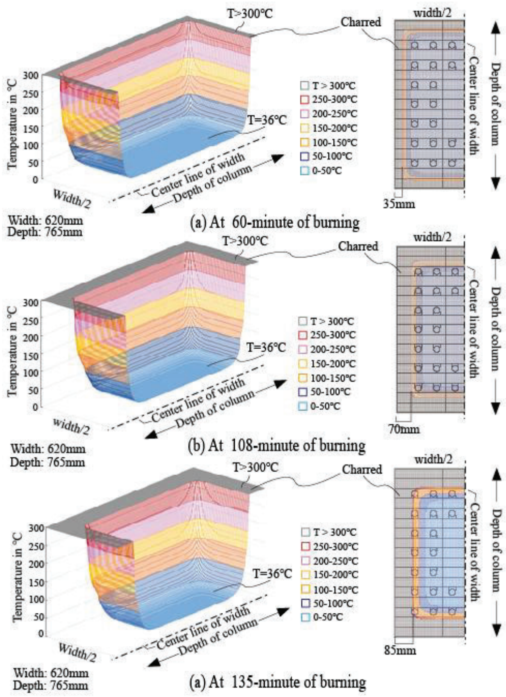

Figure 26: *Temperature profiles during burning for Specimen A1*

for the points 1 and 7 in Figure 22(c), the calculated curves(solid curves) approximately estimate the experimental curves (dotted curves).
For specimen B in Figure 22(c), the calculated curves estimate the experimental curves up to 98 minutes for the point 2 and 106 minutes for the point 8, but, ather then, for both points, the temperature increases rapidly from 140°C and reaches 960°C and 860°C, respectively, in an instant, as seen in Figure 21(c).
Such a rapid change cannot be explained by a constant charring rate. Judging from the temperature, it corresponds to the upper temperature 150°C at which the moisture in the wood evaporates and no longer has the effect of producing water vapor. Photo 7 shows the surface of the specimen after the test. Numorous cracks are observed in charred area. The cracking probaly occurs during combustion. If the thermocouple is located near the cracks, it is assumed that a rapid temperature increase occurs at the moment the cracks appear. The proposed estimation method[3] does not aim to such a sudden temperature rise. Rapid temperature increases also occur at about 250°C at the point 1 and about 220°C at the point 8 in Figure 21(a). These temperatures are close to the charring temperature and may also be influenced by variations in the charred depth. However, Young's modulus and strength of wood are significantly reduced at those temperatures, so this is not a problem in terms of estimating the strength capacity of wood. In specimen A2, the temperature of rebar was also measured; Figure 23 shows change of the temperature. The dotted cuve is the experimental curve and the solid line is the calculated curve. Cal. I is calculated as the distance of dm to the thermocouple position ・ of the rebar in Figure 23(b); Cal. II is the distance to the center of the hole in the rebar; Cal. III is the distance to the position where dm is the largest in the hole , indicated by ・ in Figure 23(b). The dotted line of the experimental curve is close to Cal. III. This indicates that the temperature rise is mitigated by the effect of the large capacity of rebar. From the point of view of ensuring strength capacity, the temperature of the rebar had better to be estimated by Equation (1) as the center of the rebar.
Figure 26 shows typical temperature profiles for the burning time of specimen A1and A2. Half of the column cross section is shown. at 60 minutes of heating, the temperature of the rebars at the periphery of the cross section was 40°C. The glass transition temperature of the adhesive for the rebar is below 67°C, and it is seemed that the rebar is still able to resist. At 135 minutes in Figure 26(c), the temperature of the outer rebar on the left side reached 250-300°C. They explain the rebar buckling at 113-130 minutes as described in Section 4.3.6.
For A2, we were able to identify vc, A, and B of the constants in Equation (1) by measuring many points where the charring temperature was reached at the combustion time, and we could confirm that the accuracy of the estimation was also high. However, we could not confirm the accuracy of the temperature with respect to B1. In order to confirm the accuracy of the temperature profile estimated by Equation (1), it is extremely important to measure seveal points where the charring temperature is reached until the combustion time.

5.5 LOADING AFTER COMPLATION OF HEATED LOADING TEST

Specimen B1 was unloaded once to near zero after a 108 minutes of heating and loading test, and extinguished with water, and the compressive force was applied again to capture its compressive strength capacity. As the upper limit load of the testing machine is 10,000 kN, the compressive force was applied up to 9,502 kN.
Fig.27 shows the relationship between compressive force and axial deformation.
The displacements were measured at four locations. The displacement transducers were initialized before reloading; the stiffness decreased at 8,800 kN; the column did not collapse axially even after applying forces up to 9,502 kN. No buckling of rebars was observed when the furnace was opened after 108 minutes of heating time, but during the reloading, rebars buckled with an impact sound and charred layer scattered. It was confirmed that the impact sound,which occurred mainly in specimen A1, was caused by the buckling of rebar.
Specimen A2 was heated for 108 minutes and the load was maintained. The furnace door was opened and the specimen was extinguished by water discharge to cool the temperature in the furnace, and the load was increased. Figure 28(a) shows the compressive force – axial deformation relationship. Figure 28(b) shows the compressive force-axial strain of the wood. The strains are the values of the wood foil gau ges that could be measured. Water from the water discharge splashed on the lead wire connections, resulting in many points where strain could not be measured. All strains on the rebar could not be measured; in Figure 28, the stiffness begins to decrease at 7,910 kN. The force began to decrease after 10 mm of deformation and 3,800 μ of strain and we confirmed the compressive stregth capacity.

https://doi.org/10.52202/080513-0119

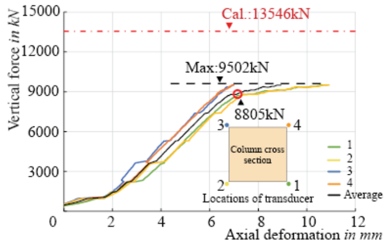

Specimen B

Figure 27: Axial force-deformation curves in reloading after burning test of B

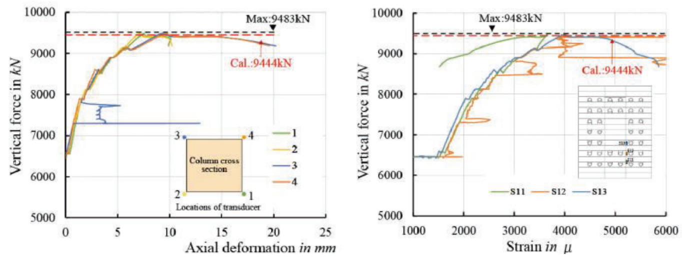

(a)Vertical force-deformation relationship (b)Vertical force-Strain relationship

***Figure 28:** Axial force-deformation curves in reloading after burning test of A2*

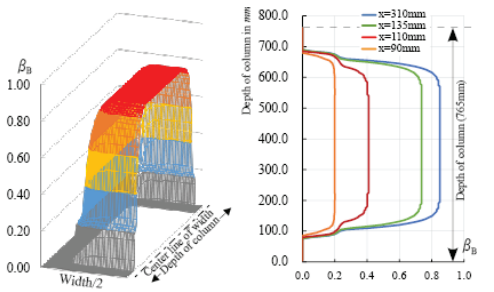

***Figure 29:** Reduction factor profile of strength of wood in cross section*

5.6 CALCULATION OF AXIAL CAPACITY

The axial compressive strength of Specimen A2 was confirmed immediately after 108 minutes of combustion. The temperature inside the specimen was also measured in detail, and based on this, the temperature profile at the 108-minute combustion was modeled. The axial compressive strength can be calculated from the temperature profile and the rate of decrease in compressive strength due to temperature rise. Shioya et al. calculated the flexural strength capcity of beams using the rate of decrease in strength due to temperature rise[3]. In the study, the rate of decrease in strength due to temperature rise was calculated using the rate of decrease in strength due to temperature rise in Eurocord 5[4]. Here, the strength reduction rate of Eurocord 5 and the compressive strength of wood and the yield strength of steel bars obtained from material test were used for the calculations. Figure 29 shows the strength reduction rate after heating for 108 minutes. This is based on the strength reduction rate of Eurocord 5. The calculated value for the capacity is shown in Figure 27 and Figure 28 as red horizontal dotted lines. B1 in Figure 27 cannot be directly compared because the axial compressive strength could not be confirmed in the experiment, but the calculated value for A2 in Figure 28 estimates the experimental value, with good accuracy.

The axial compressive strength capcity of A1 was calculated in the same way after 135 minutes of heating. The calculated capacity was 8740 kN, which is 136% of the applied load (6446 kN), so it can be confirmed that the load can be supported even after 135 minutes of combustion. These results demeosrate that the proposed estimation method for temperature profile of beam[3] can be applied to columns in the same way.

6-SUMMARY

Compression tests was conducted to determine the compression capacity of columns, including buckling capacity, and 90-minute heat test was conducted under loading. With the aim of establishing a 75-minute semi-fireproof design method for the steel bar-timber composite column, loading and heat-combustion test was conducted on three full-scale columns, assuming that three- or four-story buildings would be designed using two-way rigid frame structure made up of the composite columns and beams. The cross-sections of the columns were limited to those of the first-floor columns of three-story buildings (Column A) and four-story buildings (Column B). The results are summarized below.

1) The compression test of the column confirmed that the compression capacity of the column, including the buckling capacity, can be estimated using the slenderness ratio based on equivalent stiffness and the reduction rate of the compression capacity used in design.
2) The specimens of the composite column supported the maximun load expected in long term design for more than 108 minutes. The axial compressive strength capacity was confirmed at 108 minutes of combustion time.
3) The proposed method for estimating the internal temperature profile of a beam heated from three directions also estimated the temperature profie within columns heated and burned.
4) Assuming that the time at which the outer perimeter of the rebar inside the column buckles is the time at which the charred border reaches the rebar hole in the shortest time, it was possible to estimate the time limit for the restoration of the column on the safe side.

7– REFERENCES

[1] S. Shioya, et al.: An innovative hybrid timber structure in Japan: performance of column and beam, Wein, WCTE 2016

[2] K. Hayata, et al. : Experiement on axial capacity-bending capacity relationship of steel rebar-timber composite column, Oslo, WCTE2023

[3] S. Shioya and S. Matsushita: Estimation of temperature profile within steel bar-timber composite beam using data of combustion test, Brisben, WCTE 2025

[4] Eurocode 5, Design of timber structures - Part 1-2 General -Structural fire design, EN 1995-1-2, EUROPEAN COMMITTEE FOR STANDARD-IZATION, 2004